

# Design of a Morphable Multirotor Aerial-Aquatic Vehicle

Yu Herng Tan<sup>1</sup> and Ben M. Chen<sup>1,2</sup>

<sup>1</sup>*Department of Electrical and Computer Engineering, National University of Singapore, Singapore*

<sup>2</sup>*Department of Mechanical and Automation Engineering, Chinese University of Hong Kong, Shatin, N.T., Hong Kong*

**Abstract**—The design of any aerial-aquatic vehicle faces the unique challenge of vastly different fluid dynamics of air and water. Due to the demands of aerial propulsion, most existing solutions are fundamentally aerial vehicles with an auxiliary capability to operate underwater. Instead of using standard aerial platforms directly, we propose a novel morphable design for a multirotor-based vehicle inspired by the thruster layouts of regular aerial quadrotors and underwater remotely operated vehicles (ROVs). By adding the ability to rotate each motor about its respective arm, the proposed mechanical linkage allows for direct actuation in all six translation and rotational directions. The proposed concept is demonstrated in a proof of concept prototype and the details of the design and physical implementation are shown in this paper.

## I. INTRODUCTION

As the development of aerial and aquatic robots mature, there is an increase in their use to access areas where terrestrial robots cannot reach. Using these vehicles together will allow cross-medium functionality, which is an area of interest to many field applications. By using different robot types in different mediums to form a network of vehicles, these multi robot teams can cover vast and varying terrains. For example, such heterogeneous teams have previously been used in the aftermath survey of the Tohoku Earthquake [1], with a team that consists of remotely operated vehicles (ROVs), autonomous underwater vehicles (AUVs) and unmanned aerial vehicles (UAVs). Although this is a useful solution, multi-agent systems are inherently complex and often expensive and difficult to deploy.

Another approach to achieve similar coverage and functionality is to integrate multimodal locomotion into a single robot. Although this leads to a vehicle that is individually more complex and often involves design trade-offs to deal with the differing properties of dissimilar mediums, the ability to traverse multiple mediums with a single compact vehicle has many applications as seen in the development of road-air vehicles and the versatility and usage of amphibious vehicles in military settings.

Just as amphibious vehicles are useful in many real world terrains, the natural extension would be the development of aerial-aquatic vehicles that can operate in air and water. Although such robot functions may not seem intuitively common or useful, aerial vehicles often come within close proximity of water when operating outdoors, with applications including making use of flight to achieve fast-retrieve water sample collection [2]. Besides the ability to explore the areas and

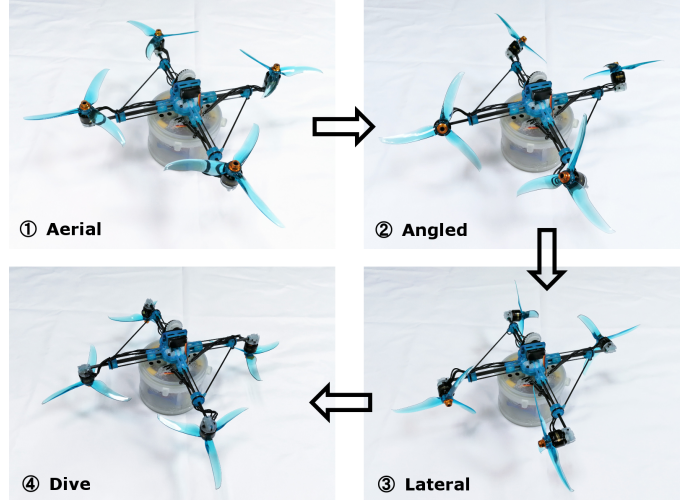


Fig. 1. The proposed morphing body for aerial-aquatic multirotors involves tilting of the four arms supporting the motors to direct thrust either vertically or laterally as needed.

terrain exclusive to water and air, such vehicles can also benefit from the property of buoyancy in water to achieve energy efficient position holding while also being able to travel at a much higher speed in air when required due to the lower surrounding fluid resistance. In addition, these vehicles would also be useful additions to cross medium teams that involve working in aerial and submerged conditions, as there is an inherent difficulty in the interface of the two mediums. Enhanced capabilities, such as being able to enter or emerge from the water surface will further increase the versatility of such teams. These potential applications have led to the development of aerial-aquatic vehicles.

In many ways, the technical demands of aerial locomotion are greater than that of water. This is mostly due to the need to generate enough lift to overcome weight in order to simply hover or hold aerial position. As such, most aerial-aquatic vehicles are primarily designed to operate in air, with an auxiliary capability to operate in water that can range from passive to fully functional. However, the opposing characteristics of the two mediums make the ability to operate efficiently in both difficult. As the density of water is almost a thousand times that of air, the dynamics and forces acting on any moving body in the two mediums will vary drastically. Furthermore, the presence of a significant buoyancy force

underwater due to this phenomenon implies that the net force acting in the gravitational direction is much lower and could possibly be positive (i.e. upwards). This leads to contradicting design requirements for an aerial-aquatic vehicle that aims to be equally adaptable in both mediums: while the weight should be minimised to maximise flight time and aerial performance, the vehicle should also be sufficiently dense to prevent significant upthrust or an external force would be required to dive underwater.

To counter the aforementioned phenomenon of opposite direction of thrust needed in the two mediums, the active thrusters of each phase has to be directed in different directions. While the simplest method of enabling this is to package two different propulsion systems, one for each medium, into a single vehicle, the additional dead weight of unused components is structurally inefficient and will further compromise the performance of aerial flight. Instead, the transition between aerial and underwater operation can be better integrated in a single platform by making use of the similarities between aerial multirotors and common underwater ROV thruster configurations. Here, the hardware structures are analysed and based on the observations, a structurally unique solution for an aerial-aquatic hybrid vehicle is proposed. The design presented features an adaptable morphing function that utilises a single propulsion system while improving the controllability of the vehicle compared to existing solutions. By using a symmetric direct linkage to achieve thrust vectoring of all motors, the proposed morphing design is mechanically simple and can be built on a small scale.

## II. BACKGROUND

Aerial-aquatic vehicles are relatively less explored compared to exclusively aerial or underwater vehicles due to the inherent complexity of operating in two mediums. They also face greater design challenges compared to amphibious vehicles due to the difficulty of navigating three-dimensional space in mediums with vastly different fluid properties. An early review of aerial-aquatic vehicles was done by Yang et. al. [3], where the authors identified three main types of aerial-aquatic vehicles: seaplane type, submersible-launched UAVs, and fully functional aquatic UAVs. The first group, seaplanes, are aerial vehicles that only come into contact with the water surface and do not venture deeper. Submersible-launched UAVs on the other hand are capable of prolonged periods of being submerged, but are otherwise passive and require external systems to transit to their primary aerial phase. Lastly, the authors identify the initial attempts at making a fully functional aerial-aquatic vehicle which can be actively self-propelled and controlled in both mediums. The majority of these are research projects in progress and there are no commercially available products of this nature currently. This is also the category that is of interest here as it involves the capability of the vehicle to operate fully both in the air and underwater, which is ultimately the goal for this class of vehicles.

Existing aerial-aquatic vehicles from this category can be classified further into two major forms: conventional multi-rotor and fixed wing vehicles. These two types of platforms vary primarily in their aerial operation, with characteristics similar to the precursor aerial counterparts that they are based on in terms of flight time and manoeuvrability. Nevertheless, the difference in hardware structure also affects the transition and operation underwater.

The existing prototypes of fixed wing aerial-aquatic vehicles function similarly to a regular fixed wing plane in air. To enter the water, they typically dive head-first directly into the target water body. The AquaMAV proposed by Siddall et. al. [4] has an additional wing folding feature that streamlines the vehicle for a smoother water entry. Two similar fixed wing prototypes were presented in [5] and [6], both of which uses flooding of the wing compartment to reduce vehicle buoyancy when underwater. While the prototypes in [5] and [7] use a single propulsion system for both air and water, [6] uses a second propeller for underwater locomotion.

The conventional quadrotor platform can be similarly adapted for underwater use by making the vehicle waterproof. The distributed nature of thrust generation in multirotors lends itself to this function as the increase in fluid forces acting on the propellers is split among the multiple thrusters. Existing aerial-aquatic quadrotors include the prototype CRACUNS [8], which is a waterproof quadrotor that can remain submerged in a hidden dormant state until it is deployed, rising to the surface and performing its task. Basic control of such vehicles underwater is then similar to that in air if the vehicle is negatively buoyant. Further enhanced prototypes of aerial-aquatic quadcopters include prototypes such as the Naviator [9] and the LoonCopter [10]. Due to the higher fluid resistance in water, these two vehicles pitch or roll at either a high angle or perpendicularly to achieve lateral movement, directing a large component of thrust in the direction of movement instead of vertically. Both of these vehicles are fully functional prototypes that operate in both air and water, with the LoonCopter using a buoyancy control system to actively adjust its buoyancy and pose to obtain the desired perpendicular angle while the Naviator uses an X8 octocopter design to the same effect. Both prototypes use aerial motors and propellers directly underwater, which is inefficient due to the torque mismatch of the system although running the motors at very low speeds can still generate sufficient thrust to steer and move the vehicle underwater.

The issue of aerial propulsion systems operating at off-design points and hence resulting in very low efficiencies is addressed in [11], in which the torque mismatch of the system is overcome by the addition of a two-mode gearbox controlled by the direction of the motor. Unlike aerial propulsion systems which spin in only one direction, underwater thrusters are often bidirectional. As most underwater vehicles are designed to be neutrally buoyant, bidirectional thrusters allow the vehicle to move directly to any desired point along the propulsion axis of the thruster without having to change the heading of the vehicle. As weight is not typically a design concern under-

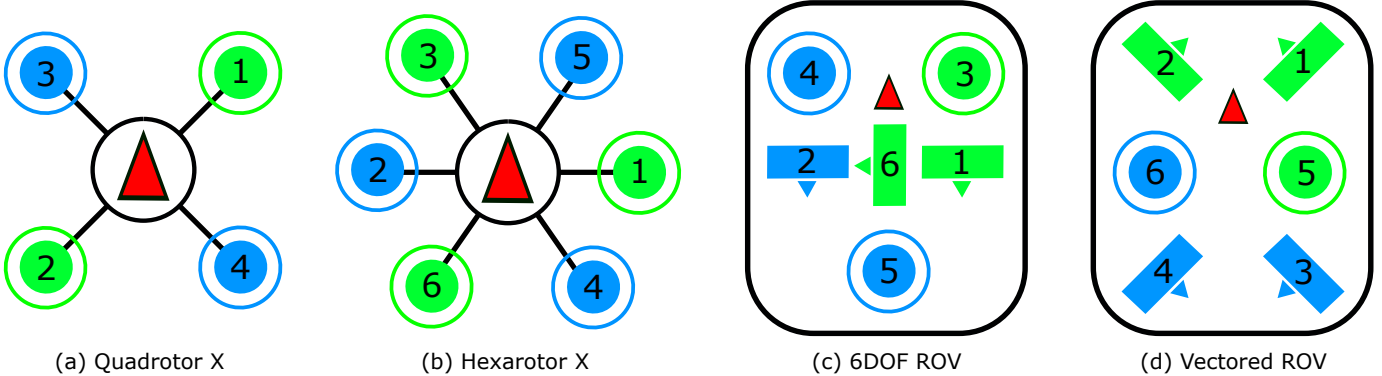


Fig. 2. Examples of typical thruster layouts for aerial multirotors (a,b) and underwater ROVs (c,d). Green indicates a counter-clockwise rotating thruster while blue represents a clockwise rotating thruster.

water, vehicles such as ROVs utilise thruster arrangements in multiple axes to obtain a fully actuated vehicle. While this is an important feature in most submersibles, no existing aerial-aquatic vehicle features such hardware configurations due to the need to satisfy aerial functionality.

From a control perspective, the ability to hover in a multirotor platform is beneficial for many applications that require precise control and movement such as manoeuvring within confined spaces. However, the current designs of aerial-aquatic quadrotors limit the control authority of the vehicle in surge, heave and sway, which are commonly the main thrust directions required when underwater. To further improve transitioning between aerial and aquatic movement, we propose a morphable body structure that can adapt the aerial multirotor platform for underwater locomotion more directly and effectively than existing solutions. In order to do so, the morphing mechanism has to be simple and sufficiently lightweight so as to not adversely affect aerial performance. Furthermore, the morphing structure has to be sufficiently rigid to maintain the structural integrity of the vehicle. These challenges are addressed in the proposed design below.

### III. THRUSTER CONFIGURATIONS

The slender torpedo-shape design of many AUVs can be seen as the underwater equivalent of a fixed wing plane. With one or more thrusters pointing in the direction of travel, this design is typically used to cover large distances at high speeds. The attitude or pose of the vehicle is controlled using control surfaces including rudders and elevators. Similarly, ROVs can be seen as the underwater equivalent of multirotors. With multiple thrusters, often positioned in a vectored configuration, ROVs are capable of precise positioning and holding its position against currents and other disturbances.

From Figure 2, we can see that the primary difference between the two types of platform lies in the way the thrusters are oriented. In aerial multirotors, all thrusters are directed vertically in the gravitational direction in order to generate lift. Rotational accelerations about each axis are then generated by varying the rotational speeds of the four rotors accordingly. As aerial vehicles face relatively low drag resistance from

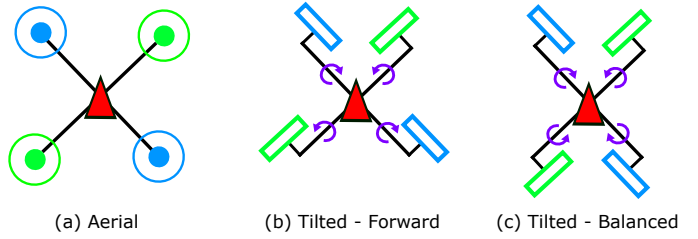


Fig. 3. The direction of tilt and the resulting configuration of a morphable body with rotating arms.

the surroundings, the small component of thrust directed in surge and sway generated by rotating the body in pitch and roll respectively is sufficient to perform lateral movement. While vertical position control is also important for ROVs, the number of thrusters acting in this axis is typically less than half of the total number of thrusters available as ROVs are usually calibrated to be neutrally buoyant and hence there is zero net force acting in the vertical direction. As vehicles in water face much larger resistance forces due to the density of the medium, most of the thrusters are typically aligned with the lateral directions, which commonly corresponds to the primary plane of motion.

The fundamental idea for the proposed design stems from the similarities in the hardware structure of these two types of vehicles. Both have rotors which are positioned so as to maximise the control authority of the vehicle in its respective medium while fulfilling basic requirements such as providing sufficient lift and maintaining equilibrium. As such, if we desire a vehicle that can operate in both mediums as effectively as these vehicles, the key would be to find a simple way of transitioning one layout to another as the vehicle moves between mediums.

In order to transition from an aerial configuration to an underwater one, the primary change needed is to rotate the thrusters to act in the desired axis. This can be done on a quadrotor platform by tilting the arm that each rotor sits on by 90 degrees. At the same time, this extra input variable of the tilt mechanism allows the set of monodirectional thrusters

to act in the opposite direction, hence avoiding the need to rotate the entire vehicle body frame or relying on extra sets of thrusters.

The actuation of this tilting can be simplified if the rotors tilt symmetrically. There are two basic intuitive ways which this can be done, as shown in Figure 3. If each perpendicular cross-arm of the quadrotor rotated in one direction, this would result in the *forward* configuration shown in Figure 3b, while if each end of the cross-arm twisted in the opposite direction, the resulting configuration would be the *balanced* configuration shown in Figure 3c.

Although the thrusters, when rotated perpendicularly, are not acting directly in the surge, heave and sway directions, the angle implies that a component of thrust from each thruster will act in each of these directions. This is similar to the vectored thruster layout in ROVs (Figure 2d). The balanced configuration (Figure 3c) is symmetric about both roll and pitch axes, while the forward configuration (Figure 3b) is only symmetric about the roll axis. However, in the balanced layout, only the two front thrusters can be used for forward propulsion. The forward layout overcomes this by pointing the thrusters in the same general lateral direction. However, the cost of doing so is the ability to hold position without tilting of thrusters. With each pair of thrusters pointing in opposite directions, the balanced layout is more effective in correcting for hovering uncertainties in the lateral plane.

Here, the balanced tilting configuration was chosen to be further investigated as a symmetric layout in all three rotational axes simplifies several considerations while also being mechanically simpler to implement, which will be discussed further in Section V.

#### IV. VEHICLE DYNAMICS MODELLING

To understand the effect of the thruster tilting mechanism on the dynamics of the vehicle, we first look at the general model of a standard aerial quadrotor, which can be given in the widely used local North-East-Down (NED) positional frame  $\mathbf{F}_n$ . The body frame  $\mathbf{F}_b$  is defined as an origin located at the centre of gravity of the full system, with  $\mathbf{X}_b$  pointing towards the front of the system,  $\mathbf{Y}_b$  pointing towards the right and  $\mathbf{Z}_b$  pointing downwards. The position of the full system in  $\mathbf{F}_n$  is defined as  $\mathbf{P}_n = [x, y, z]^T$ , and the orientation in  $\mathbf{F}_n$  is defined by the Euler angles  $\Theta = [\phi, \theta, \psi]^T$ . The body frame velocity and body frame angular velocity are expressed as  $\mathbf{V}_b = [u, v, w]^T$  and  $\omega_b = [p, q, r]^T$  respectively. The rotational and translational motions between the global and body coordinates are then given by the following navigation equations [12]:

$$\dot{\mathbf{P}}_n = \mathbf{R}_{n/b} \mathbf{V}_b \quad (1)$$

$$\dot{\Theta} = \mathbf{S}^{-1} \omega_b \quad (2)$$

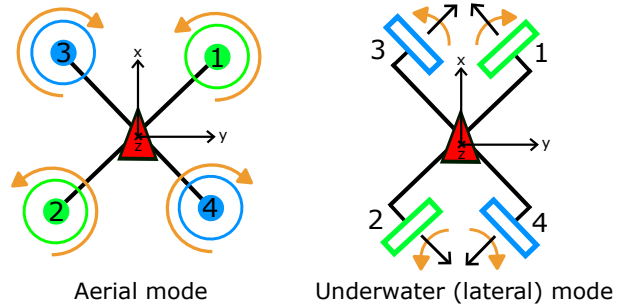


Fig. 4. The indices and direction of the rotors.

where the rotational matrix  $\mathbf{R}_{n/b}$  and lumped transformation matrix  $\mathbf{S}^{-1}$  are

$$\mathbf{R}_{n/b} = \begin{bmatrix} c_\theta c_\psi & s_\phi s_\theta c_\psi - c_\phi s_\psi & c_\phi s_\theta c_\psi + s_\phi s_\psi \\ c_\theta s_\psi & s_\phi s_\theta s_\psi + c_\phi c_\psi & c_\phi s_\theta s_\psi - s_\phi c_\psi \\ -s_\theta & s_\phi c_\theta & c_\phi c_\theta \end{bmatrix} \quad (3)$$

$$\mathbf{S}^{-1} = \begin{bmatrix} 1 & s_\phi t_\theta & c_\phi t_\theta \\ 0 & c_\phi & -s_\phi \\ 0 & s_\phi/c_\theta & c_\phi/c_\theta \end{bmatrix} \quad (4)$$

and  $s_* = \sin(*)$ ,  $c_* = \cos(*)$  and  $t_* = \tan(*)$ . The rigid body dynamics can then be expressed as

$$\dot{\mathbf{V}}_b = \frac{1}{m} \mathbf{F}_b - \omega_b \times \mathbf{V}_b \quad (5)$$

$$\dot{\omega}_b = \mathbf{I}^{-1} (\mathbf{M}_b - \omega_b \times \mathbf{I} \omega_b) \quad (6)$$

where  $\mathbf{F}_b$  and  $\mathbf{M}_b$  are the net force and moments generated by the UAV. As the system is symmetric, the inertia matrix  $\mathbf{I}$  is diagonal and  $I_{xx} = I_{yy}$ .

$$\mathbf{I} = \begin{bmatrix} I_{xx} & 0 & 0 \\ 0 & I_{yy} & 0 \\ 0 & 0 & I_{zz} \end{bmatrix} \quad (7)$$

1) *Aerial quadrotor*: For a standard quadrotor with configuration shown in Figure 4, the force and moment vectors can be expressed as:

$$\mathbf{F}_b = \begin{bmatrix} 0 \\ 0 \\ |T_1| + |T_2| + |T_3| + |T_4| \end{bmatrix} + mg \begin{bmatrix} -\sin \theta \\ \sin \phi \cos \theta \\ \cos \phi \cos \theta \end{bmatrix} \quad (8)$$

$$\mathbf{M}_b = \begin{bmatrix} \frac{l}{\sqrt{2}} (|T_2| + |T_3| - |T_1| - |T_4|) \\ \frac{l}{\sqrt{2}} (|T_1| + |T_3| - |T_2| - |T_4|) \\ M_1 + M_2 - M_3 - M_4 \end{bmatrix} \quad (9)$$

$T_i$  and  $M_i$  are the lift and torque generated by the  $i^{\text{th}}$  motor respectively and can be expressed as:

$$T_i = K_T \omega_i^2 \quad (10)$$

$$M_i = K_M \omega_i^2 \quad (11)$$

where  $\omega_i$  is the rotating speed of the motor and  $K_T$  and  $K_M$  are the constant coefficients of the propeller used which can be determined experimentally. The rotating speed of the

motor  $\omega_i$  and the input signal  $\delta_i$  (scaled to [0 1]) follows the relationship [13]:

$$\omega_i(s) = \frac{C_m}{1 + \tau_i s} \delta_i(s) \quad (12)$$

where  $C_m$  is the motor rotating speed coefficient and  $\tau_i$  is the time constant of the motor response.

2) *Proposed underwater configuration:* With the proposed tilting mechanism, we now have an additional input variable of the tilt angle,  $\beta$ , where  $-\pi/2 \leq \beta \leq \pi/2$  will allow full actuation of the vehicle as described above. As the rotation is directly linked, the tilt angle of each thruster will be the same, although the direction will depend on the arm axes. For the balanced configuration, we define the tilt angle such that  $\beta = 0$  implies the vehicle is in full lateral mode while  $\beta = \pi/2$  implies that the vehicle is in regular aerial mode. The labels and directions of the motors are shown in Figure 4.

The force and moments in the proposed balanced configuration can then be written as

$$\mathbf{F}_b = \begin{bmatrix} \frac{\sqrt{2}}{2} \cos \beta (|T_1| - |T_2| + |T_3| - |T_4|) \\ \frac{\sqrt{2}}{2} \cos \beta (-|T_1| + |T_2| + |T_3| - |T_4|) \\ \sin \beta (|T_1| + |T_2| + |T_3| + |T_4|) \end{bmatrix} + (mg - U) \begin{bmatrix} -\sin \theta \\ \sin \phi \cos \theta \\ \cos \phi \cos \theta \end{bmatrix} \quad (13)$$

$$\mathbf{M}_b = \begin{bmatrix} \frac{l}{\sqrt{2}} \sin \beta (-|T_1| + |T_2| + |T_3| - |T_4|) \\ \frac{l}{\sqrt{2}} \sin \beta (|T_1| - |T_2| + |T_3| - |T_4|) \\ \frac{l}{\sqrt{2}} (-T_1 + T_2 + T_3 - T_4) \end{bmatrix} + \sum_i^4 \begin{bmatrix} M_{iX} \\ M_{iY} \\ M_{iZ} \end{bmatrix} \quad (14)$$

Where  $U$  is the buoyancy force and  $M_{iX}$ ,  $M_{iY}$ ,  $M_{iZ}$  represent the moment in the  $X$ ,  $Y$ ,  $Z$  axis caused by the rotation of the  $i^{th}$  motor. Considering the relatively low rotational speeds of the motors in water, this value is likely to be small and negligible.

We can see from the formulation above that the addition of the tilt angle variable enables direct actuation in all six translational and rotational directions. Although the system appears highly coupled and complex compared to a regular aerial quadrotor, the use of the tilt angle  $\beta$  allows the system to be greatly simplified when  $\beta = 0$ ,  $\beta = \pi/2$  and  $\beta = -\pi/2$ . At latter two points, which correspond to the normal aerial mode (all motors pointing upwards) and dive mode (all motors pointing downwards) respectively, the thrusters only affect one translational direction while at  $\beta = 0$ , which corresponds to the lateral travel mode, thruster speeds do not affect roll and pitch. This makes the vehicle structure versatile for a variety of control strategies, allowing simple direct actuation while also capable of implementing more complex coupled manoeuvres.

As a further extension to the proposed idea, a fully decoupled 6 degree-of-freedom (DOF) vehicle can theoretically be designed using a +octocopter layout with four of the rotors on the 'X' arm tiltable as in the case discussed above, in which case the variable  $\beta$  will no longer be required as a control input and the tilting of the rotors (from  $\beta = \pi/2$  to  $\beta = 0$ ) is

only activated during the transition from aerial to underwater mode. The fundamentals of such a design, however, will be similar to the quadrotor layout that is discussed further below.

## V. MECHANICAL DESIGN

Since the tilting of the rotors are symmetric and does not need to be decoupled, this action can be controlled by a single actuator with a mechanical linkage to enable this. Four inward facing mitre gears (Figure 5), each connected to one arm of the quadrotor, will be able to achieve the effect of balanced tilting described above. This is considerably simpler than implementing the forward tilting configuration shown in Figure 3b. For the centres of the two cross arms to remain aligned while the counter-rotating requirements are fulfilled, only one of the two perpendicular cross arms can be connected on a single shaft although all four arms are rotating in the same direction as the respective opposite arm. To connect the other two arms, a similar mitre gear drive as above can be used. However, for the arms to rotate in the desired direction, each pair of mitre gears must not cross-interact with the drive in the opposite direction. In order to keep the 1:1 drive ratio and the mechanism on a single plane each mitre gear has to be modified into a half gear. The alternative would be to stagger the drive shafts in two horizontal planes, which will result in a more mechanically complicated and hence heavier structure.

Another consideration when implementing this concept is the sizing and clearance needed for the rotors. For a general multirotor, the minimum wheelbase (motor to motor distance) is dependent on the size of the propeller used. The minimum allowable half-wheelbase or wheelbase radius,  $R$ , can be expressed as

$$R \geq \frac{\sigma}{\sin(\alpha/2)} r_P \quad (15)$$

where  $r_P$  is the radius of the propeller,  $\alpha$  is the angle between adjacent arms given by  $\alpha = 2\pi/n$  for a multirotor with  $n$  number of arms and  $\sigma$  is the safety factor. For a quadrotor, this requirement is  $R \geq \sigma\sqrt{2}r_P$ . However,  $R$  could also be restricted by the minimum hub area required, in which case  $R$  must also satisfy

$$R \geq \sigma(r_P + r_H) \quad (16)$$

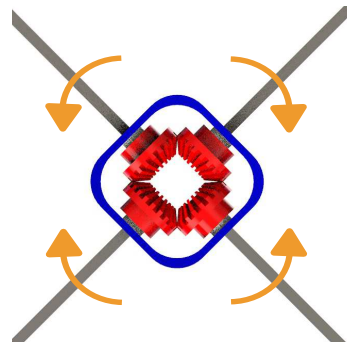


Fig. 5. The simple mechanism using four mitre gears showing the relative direction of rotation for each arm.

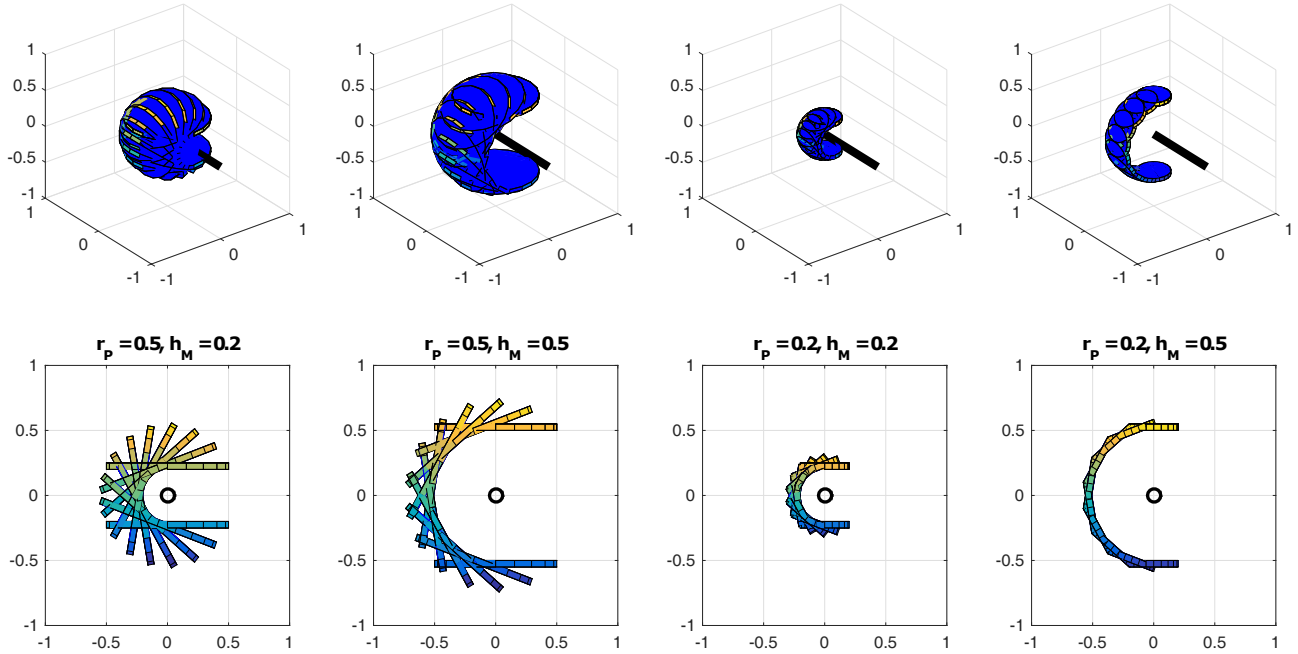


Fig. 6. Visualisation of the clearance volume needed for various values of  $r_P$  and  $h_M$ . The second row shows the cross-sectional view looking into the arm axis.

where  $r_H$  is the radius of the hub.

In the proposed design, the rotors will rotate about the axis of each arm, further increasing the clearance volume required. As the clearance space needed is any positional space that the spinning rotors occupy under the possible tilt settings, the height of the propeller disc plane from the centre of the arm becomes a key parameter. This can be seen as the eccentricity about which the propeller disc is rotated about the arm axis. The degree of rotation corresponds with the range of arm rotation. Considering a general 360 degree rotation, the external clearance volume,  $V$ , will be an ellipsoid given by

$$V = \frac{4}{3}\pi(r_P^2 + h_M^2)r_P \quad (17)$$

about the arm axis where  $h_M$  is the eccentricity, physically represented by the distance between the propeller plane and the centre of the arm. For the case where  $-\pi/2 \leq \beta \leq \pi/2$  as defined above, a visualisation of the clearance required for different eccentricities and propeller radii is shown in Figure 6. Besides ensuring no structural elements such as the frame or landing gear intersect with volume, the prop-to-prop clearance required by this tilting can be simplified to

$$R \geq \sigma(r_P + h_M) \quad (18)$$

which will typically be satisfied if Equation 16 is satisfied since the motor heights are usually much smaller than the hub radius.

## VI. INITIAL PROTOTYPE DEVELOPMENT

A small scale prototype (Figure 7) was built as a proof of concept of the proposed design. The scale of the demonstrated prototype was chosen for cost considerations and ease of manufacturing, though no part of the design prohibits scalability and hence can be similarly built on a larger scale. The prototype was sized according to a 5-inch propeller and weighs 425.7 g. Using a safety factor of  $\sigma = 1.1$ ,  $r_P = 75\text{mm}$ , and  $r_H = 45\text{mm}$ , the minimum wheelbase of 264 mm was used. Activating the tilting mechanism with  $-\pi/2 \leq \beta \leq \pi/2$  results in the configurations shown in Figure 1.

The propulsion system used include T-MOTOR F20II-3750KV motors paired with T5143 3-blade propellers. These



Fig. 7. The first prototype of the proposed design.

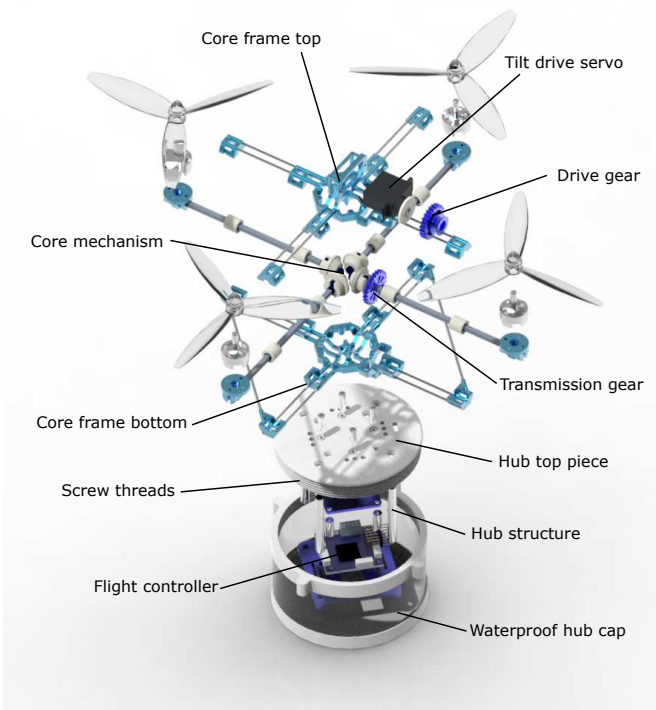


Fig. 8. Exploded view of the prototype design rendered in CAD.

TABLE I  
MASS BREAKDOWN OF THE PROTOTYPE COMPONENTS.

Component	Mass (g)
Motors	60.8
ESCs	20.4
Propellers	15.2
Flight controller	10.5
PDB	7.0
Receiver	4.0
Tilt drive servo	9.0
Core frame and mechanism	94.3
Hub structure	55.3
Waterproof hub cap	50.2
Battery	85.0
Wiring & fixtures	14.0
<b>Total</b>	<b>425.7</b>

are driven by four 21 A electronic speed controllers (ESCs) and controlled using a Pixracer R15 flight controller. With a 1300 mAh 2S lithium-polymer battery, a thrust-to-weight ratio of 2.9 can be achieved with this setup. A Holybro PM06 power distribution board (PDB) provides the power supply and a standard 9 g servo with 180 degree rotation was used for the tilt mechanism. The mass breakdown of the components is shown in Table I.

The basis of the design revolves around the core mechanism described in Section V, which mechanically connects the four arms to rotate in the desired direction. This mechanism is driven by a single servo actuator that is able to rotate 180 degrees. Although gearing can allow a servo with less travel to achieve the desired tilt, the tilt drive mechanism uses a 1:1 drive ratio to maintain sufficient torque as well as to not dilute



Fig. 9. Details of the core mechanism in the built prototype.

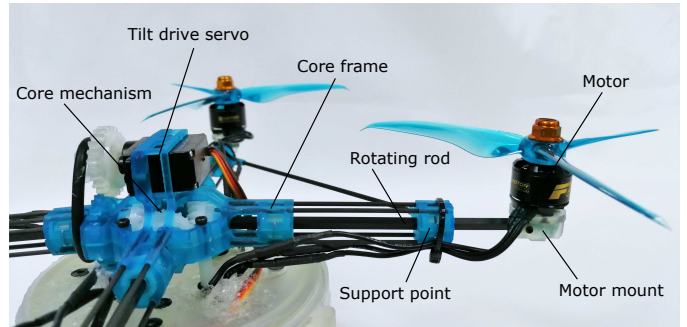


Fig. 10. Details of the rotating arm shaft in the built prototype.

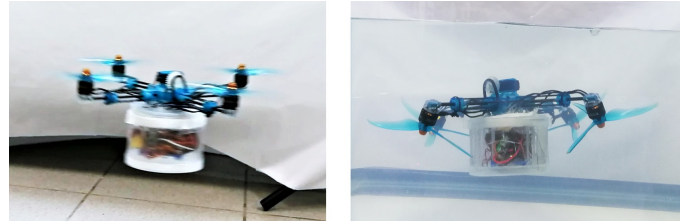


Fig. 11. Testing of the prototype in air (L) and water (R).

the resolution of the servo control. To minimise the backlash of the gears which will cause unwanted displacement and uncertainty in the tilt angle, The servo drive gear is elastically held in tension to the connecting transmission gear.

As shown in Figure 8, the rotating rod of each arm is built individually and contained within the core frame, forming the core mechanism. To support these arms, the core frame, 3D printed using stereolithography (SLA), is strengthened with 1.5 mm diameter carbon fibre rods which extend out to a secondary support point near the motor mounts on each arm. This is necessary as the arms, which typically define the frame structure and is fundamental to ensuring the vehicle's rigidity, are not only separate individual pieces here but are also required to rotate. Each of these secondary support points are also further connected to one adjacent support point to increase the rigidity of the structure. The choice to rotate the arms 180 degrees in one direction instead of a full 360 degrees not only avoids redundancy but also allows an area (shown in Figure 6) where this structural support can be anchored. The core frame is built in two halves which encloses the rods and gears securely while allowing rotational movement. To ensure smooth rotation of the arms, ABS spacers along the rotating

rods act as a buffer between the frame and the rods. The drive servo sits on top of the core mechanism and is linked via a single transmission gear on one of the arms. The details of resulting build are pictured in Figures 9 and 10.

As defined in the clearance requirements above, the hub size  $r_H$  corresponds to a cylindrical volume around the centre of the vehicle where the electronic components of the vehicle can be placed. Here, the hub makes full use of this cylindrical space to hold the electronics within a waterproof container. This container was designed as a separate piece under-slung from the core mechanism to allow the core to be a separate assembly for the prototyping process. The components in the core assembly (i.e. outside the hub) are also those which can either be individually waterproofed (servo) or do not require waterproofing (gears, propellers and brushless outrunner motors).

Ensuring watertightness of the hub is a major challenge especially when weight is a concern. In addition, the container should allow easy access to the components for maintenance and powering up of the vehicle. As such the sealed cylinder is designed as two pieces: the top piece, which is mounted under the core, and the bottom cap, which is a plastic cover that surrounds the body. The top piece contains a skeletal structure which holds the electronic components rigidly, while the bottom cap goes over this structure and screws into the top piece, forming a single cylinder that is easily accessible. The screwcap design for the large diameter hub uses a standard unified thread with a 2 mm pitch. The pieces were printed using SLA with 50 micron layer thickness and properly mated despite residual defects from removing of supports. PTFE tape further strengthened the watertightness of the thread. The top piece has holes through which the ESC and external servo wires are inserted and sealed using silicone.

The prototype was tested and able to execute aerial flight as a regular quadrotor with  $\beta = \pi/2$ . Water testing also verified the waterproofing of the sealed cylinder and basic propulsion underwater. The current prototype is controlled manually using direct actuation. Ongoing work continues to investigate the control and actuator mixing possibilities to fully exploit the advantages of thrust vectoring. Furthermore, this prototype is positively buoyant and hence require a constant value of  $\beta < 0$  to dive beneath the water surface. Although functional, this is not efficient. The estimated upthrust of the vehicle from volume analysis is around 4.5 N, which is only slightly more than the total weight. Hence, this can be rectified in future prototypes by reducing the hub volume further to ideally obtain neutral buoyancy.

## VII. CONCLUSION

The work here presents the initial design and analysis of a unique hardware structure that functionally adapts a standard aerial quadrotor into an aerial-aquatic vehicle. The idea based on the thruster layout and configuration of typical aerial and underwater vehicles is discussed and a mechanical implementation of the concept is shown. The physical design constraints of such a vehicle are also discussed as it is unlike

any existing prototypes. A proof of concept prototype shows that the proposed idea is feasible and can be applied on a small scale.

This paper covers the basic concept and development, though there are several areas which still require further work to fully realise the potential of the platform. Currently, the actuator mixing uses the default quadrotor configuration with minor adaptations for the lateral mode function. The versatility of the platform allows for interesting alternatives in actuator mixing and thruster allocations to achieve characteristics and performances as desired. The prototype presented also uses a single aerial propulsion system for both air and water. Although basic simulations verified that the chosen configuration is safe and feasible, it has not been optimised. Future work includes a study that aims to characterise an optimal scale or strategy to improve aerial propulsion performance underwater.

## REFERENCES

- [1] R. R. Murphy, K. L. Dreger, S. Newsome, J. Rodocker, B. Slaughter, R. Smith, E. Steimle, T. Kimura, K. Makabe, K. Kon, H. Mizumoto, M. Hatayama, F. Matsuno, S. Tadokoro, and O. Kawase, "Marine heterogeneous multirobot systems at the great Eastern Japan Tsunami recovery," *Journal of Field Robotics*, vol. 29, no. 5, pp. 819–831, sep 2012. [Online]. Available: <http://doi.wiley.com/10.1002/rob.21435>
- [2] J.-P. Ore, S. Elbaum, A. Burgin, and C. Detweiler, "Autonomous Aerial Water Sampling," *Journal of Field Robotics*, vol. 32, no. 8, pp. 1095–1113, dec 2015. [Online]. Available: <http://doi.wiley.com/10.1002/rob.21591>
- [3] X. Yang, T. Wang, J. Liang, G. Yao, and M. Liu, "Survey on the novel hybrid aquaticaerial amphibious aircraft: Aquatic unmanned aerial vehicle (AquaUAV)," *Progress in Aerospace Sciences*, vol. 74, pp. 131–151, apr 2015.
- [4] R. Siddall, A. Ortega Ancel, and M. Kovac, "Wind and water tunnel testing of a morphing aquatic micro air vehicle," *Interface Focus*, vol. 7, no. 1, feb 2017. [Online]. Available: <http://rsfs.royalsocietypublishing.org/lookup/doi/10.1098/rsfs.2016.0085>
- [5] W. Weisler, W. Stewart, M. B. Anderson, K. J. Peters, A. Gopalaraman, and M. Bryant, "Testing and Characterization of a Fixed Wing Cross-Domain Unmanned Vehicle Operating in Aerial and Underwater Environments," *IEEE Journal of Oceanic Engineering*, vol. 43, no. 4, pp. 969–982, oct 2018.
- [6] W. Stewart, W. Weisler, M. MacLeod, T. Powers, A. Defreitas, R. Gitter, M. Anderson, K. Peters, A. Gopalaraman, and M. Bryant, "Design and demonstration of a seabird-inspired fixed-wing hybrid UAV-UUV system," *Bioinspiration & Biomimetics*, vol. 13, no. 5, aug 2018.
- [7] J. Moore, A. Fein, and W. Setzler, "Design and Analysis of a Fixed-Wing Unmanned Aerial-Aquatic Vehicle," in *2018 IEEE International Conference on Robotics and Automation (ICRA)*. IEEE, may 2018, pp. 1236–1243.
- [8] G. Brown, "New UAV Can Launch from Underwater for Aerial Missions," *John Hopkins Applied Physics Laboratory*, 2016.
- [9] M. M. Maia, P. Soni, and F. J. Diez-Garias, "Demonstration of an Aerial and Submersible Vehicle Capable of Flight and Underwater Navigation with Seamless Air-Water Transition," *arXiv*, 2015.
- [10] H. Alzu'bi, I. Mansour, and O. Rawashdeh, "Loon Copter: Implementation of a hybrid unmanned aquatic-aerial quadcopter with active buoyancy control," *Journal of Field Robotics*, vol. 35, no. 5, pp. 764–778, Aug 2018.
- [11] Y. H. Tan, R. Siddall, and M. Kovac, "Efficient AerialAquatic Locomotion With a Single Propulsion System," *IEEE Robotics and Automation Letters*, vol. 2, no. 3, pp. 1304–1311, jul 2017. [Online]. Available: <http://ieeexplore.ieee.org/document/7847338/>
- [12] G. Cai, B. M. Chen, and T. H. Lee, *Unmanned Rotorcraft Systems*, ser. Advances in Industrial Control. London: Springer London, 2011.
- [13] L. Wu, Y. Ke, and B. M. Chen, "Systematic Modeling of Rotor Dynamics for Small Unmanned Aerial Vehicles," in *International Micro Air Vehicles Competition and Conference*, Beijing, China, 2016, pp. 284–290.